

A composite measurement scheme for efficient quantum observable estimation

Zi-Jian Zhang,^{1,2} Kouhei Nakaji,^{3,4,5} Matthew Choi,^{1,2} and Alán Aspuru-Guzik^{3,1,2,6,7,8,*}

¹*Department of Computer Science, University of Toronto, Toronto, Ontario M5S 2E4, Canada*

²*Vector Institute for Artificial Intelligence, Toronto, Ontario M5S 1M1, Canada*

³*Department of Chemistry, University of Toronto, Toronto, Ontario M5G 1Z8, Canada*

⁴*Research Center for Emerging Computing Technologies, National Institute of Advanced Industrial Science and Technology (AIST), 1-1-1 Umezono, Tsukuba, Ibaraki 305-8568, Japan*

⁵*Quantum Computing Center, Keio University, 3-14-1 Hiyoshi, Kohoku-ku, Yokohama, Kanagawa, 223-8522, Japan*

⁶*Department of Materials Science & Engineering, University of Toronto, Toronto, Ontario M5S 3E4, Canada*

⁷*Department of Chemical Engineering & Applied Chemistry, University of Toronto, Toronto, Ontario M5S 3E5, Canada*

⁸*Lebovic Fellow, Canadian Institute for Advanced Research, Toronto, Ontario M5G 1Z8, Canada*

(Dated: May 5, 2023)

Estimation of the expectation value of observables is a key subroutine in quantum computing and is also the bottleneck of the performance of many near-term quantum algorithms. Many works have been proposed to reduce the number of measurements needed for this task and they provide different measurement schemes for generating the measurements to perform. In this paper, we propose a new approach, composite measurement scheme, which composes multiple measurement schemes by distributing shots to them with a trainable ratio. As an example of our method, we study the case where only Pauli measurements are allowed and propose Composite-LBCS (C-LBCS), a composite measurement scheme made by composing locally-biased classical shadows. We numerically demonstrate C-LBCS on molecular systems up to CO₂ (30 qubits) and show that C-LBCS outperforms the previous state-of-the-art methods despite its simplicity. We also show that C-LBCS can be efficiently optimized by stochastic gradient descent and is trainable even when the observable contains a large number of terms. We believe our method opens up a reliable way toward efficient observable estimation on large quantum systems.

I. INTRODUCTION

Quantum technology makes it possible to create and measure entangled quantum states living in high-dimensional Hilbert spaces, enabling the implementation of quantum algorithms fundamentally faster than their classical counterparts [1–3]. In these algorithms, the measurement of quantum states plays a critical role. On one hand, it converts intangible quantum states to classical results that can be recognized and serve as outputs. On the other hand, the destructive nature of quantum measurements forces one to prepare the quantum states multiple times, forming the bottleneck of many quantum applications. Significantly, the emergence of near-term intermediate-scale quantum (NISQ) devices [4, 5] puts efficient measurement methods in increasing importance since near-term quantum algorithms typically involve estimating the expectation value of complicated observables [5–11]. There are also error mitigation methods [8, 12–14] proposed for trading the number of measurements with the accuracy of the result, making measurement methods a significant factor in the overall performance of near-term algorithms.

The problem of estimating the expectation value of observables on a quantum state can be formulated as follows: there is an observable $O = \sum_j a_j O_j$, where \vec{a} are real coefficients and $\{O_j\}$ are easily measurable fragments of the observable O . Given a quantum state $|\psi\rangle$ that we can prepare, the problem is how to estimate the expectation value $\langle O \rangle = \langle \psi | O | \psi \rangle$ to a certain accuracy with fewer copies (shots) of $|\psi\rangle$. We note

that for quantum computing with near-term quantum devices, we usually limit the family of measurements to Pauli measurements so that they can be easily implemented; correspondingly, the observable is decomposed into a sum of the tensor product of Pauli operators (Pauli strings) as $O = \sum_j a_j P_j$. If one naively estimates the expectation value by independently performing the estimation on each Pauli string, to a fixed accuracy, the required number of measurements scales quadratically with $\|\vec{a}\|_1$. This will be problematic when larger systems of practical interest are considered.

Various measurement methods have been proposed to mitigate the problem above and there are roughly two important families of them. The first family outputs a probability distribution on a small set of measurements for a given observable. The measurements to be made can then be sampled from the set. The methods in the family can be represented by the largest degree first (LDF) grouping [15], overlapped group measurement (OGM) [16], and other recent approaches [17, 18]. An additional large family of methods is characterized by using ideas from classical shadow (CS) [19] and locally-biased classical shadow (LBCS) [20]. These methods are not associated with a small set of measurements to sample from. Instead, they employ distributions on all Pauli measurements. This family of methods provides a feasible way to measure the observables even when they contain exponentially many terms [19]. However, these methods usually only offer distributions of measurements with a simple structure and cannot provide the best performance for molecular Hamiltonians [16]. This drawback makes them currently not the best choice for applications such as variational quantum eigensolver (VQE) [7]. Therefore, how to enhance the representation power of these methods so that they have a bet-

* aspuru@utoronto.ca

ter shot efficiency for complicated observables, becomes an interesting question.

In this work, we introduce a new approach, the composite measurement scheme, for designing efficient measurement methods. The composite measurement scheme combines multiple measurement generators (measurement schemes) together by a weighted combination of them. Based on this methodology, we are able to scale up a type of measurement scheme by combining many of them. As an example of our methodology, we study a method we call the composite-LBCS (C-LBCS), which combines multiple LBCS schemes. We numerically show that by optimizing the weights of the combination and the parameters in each LBCS scheme together, with a gradient rescaling strategy and a two time-scale update rule (TTUR) [21], the combined measurement scheme can provide state-of-the-art measurement efficiency, even when stochastic gradient descent with a small batch size is adopted.

The rest of the paper is organized as follows. In Sec. II, we present the framework and our methodology. Then, in Sec. III, we propose several optimization strategies that are tailored to our case. In Sec. IV, we demonstrate a specific method (C-LBCS) that is based on our methodology and compare its performance with previous methods on various molecule Hamiltonians. Finally, in Sec. V, we conclude with discussion and a general outlook.

II. FRAMEWORK

A. Measurement schemes

In this work, we define the term *measurement schemes* (MS) as measurement generators that input the required number of measurements and output a set of measurements to perform.

Definition 1 (Measurement scheme). *A measurement scheme S is a generator of measurements that outputs a multi-set of measurements on the objective quantum system given the required number of measurements (shot number) and optionally other information.*

A measurement scheme may contain optimizable parameters. For example, in the LBCS method [20], the probabilities of generating each Pauli operator on each qubit are the parameters to be optimized. In OGM [16], the parameters are the probabilities of generating each Pauli measurement (group) that is constructed by the method. We note that we formulate these optimizable parameters as included within a measurement scheme rather than provided as inputs.

Here, we emphasize the difference between the term *measurement scheme* and the term *measurement method*. By *measurement method*, we imply it is an end-to-end protocol for estimating the expectation value of observables, which includes the optimization of the parameters, the measurements generation, the measurements process and the post-processing protocol that synthesizes the final result from measurement outcomes. In this sense, previously proposed methods such as OGM [16] and LBCS [20] can be recognized as measurement

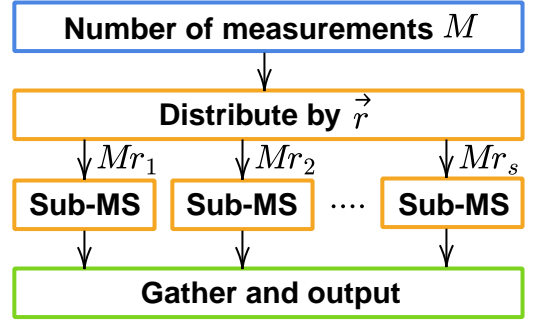


FIG. 1. A diagrammatic representation of the composite measurement scheme defined in Definition 3. The total number of measurements M is distributed to sub-measurement-schemes (Sub-MS) by the probabilities \vec{r} . The composite scheme gathers the measurements generated by all the sub-schemes as the output.

methods that contain a measurement scheme. Measurement schemes, on the other hand, are just generators of measurements. Based on this definition, there is a special family of measurement schemes that has a memory-less (Markovian) structure.

Definition 2 (Simple measurement scheme). *A simple measurement scheme S is a measurement scheme that can be implemented by sampling measurements from a fixed distribution for each required measurement.*

A simple measurement scheme only inputs the number of measurements needed and the generation of each measurement is independent. Many proposed measurement schemes (e.g. the ones used in OGM and LBCS) can be modelled by simple measurement schemes and their simple structure makes them easy to analyze and serve as a base for generalization.

B. Composite measurement schemes

Next, we introduce a way to combine multiple simple measurement schemes to make a *composite measurement scheme* (CMS). Suppose \vec{S} is a list of schemes to be combined. A natural way to combine multiple schemes is to assign each scheme a probability; when generating a measurement from the combined scheme, we sample a scheme according to the probability and generate a measurement from the sampled scheme. Specifically, we propose the SampleProd operator to represent this combination.

Definition 3 (Composite measurement scheme). *Suppose there is a list of simple measurement schemes \vec{S} and there is a distribution of the schemes in \vec{S} represented by the probabilities \vec{r} , in which r_k corresponds to S_k . We define $S' = \text{SampleProd}(\vec{r}, \vec{S})$ to be the composite measurement scheme which generates each measurement by first sampling a sub-scheme $S_{k'}$ from \vec{S} by the probabilities \vec{r} and then generating a measurement from $S_{k'}$.*

CMS can be used to form interesting new types of measurement schemes. For example, it is viable to combine shadow methods with grouping methods by making SampleProd of their measurement schemes.

More importantly, CMS provides a way to scale up measurement schemes. In this work, we will focus on demonstrating SampleProd by applying it to LBCS schemes as an example of CMS. The measurement scheme of LBCS has a distribution β_i on the set of Pauli operators (X, Y and Z) for each qubit i in the system. When generating a measurement, for the i -th qubit, the scheme samples a Pauli operator on the qubit by the distribution β_i . The Pauli measurement generated will be the tensor product of the Pauli operators sampled for each qubit. Suppose \vec{S} is a list of LBCS schemes, SampleProd(\vec{r}, \vec{S}) offers a natural generalization of single LBCS schemes, which we call by composite-LBCS (C-LBCS) in this work.

Protocol 1: Composite locally-biased classical shadow (C-LBCS)

1. Suppose the composite scheme is made by SampleProd(\vec{r}, \vec{S}), in which each sub-scheme S_k is a LBCS scheme with adjustable distributions $\{\beta_i^k\}$.
 2. When M measurements are required, repeat the following process M times.
 - Sample a sub-scheme $S_{k'}$ by the probabilities \vec{r} . Initialize a Pauli string Q with $Q[i] = I$ for all i .
 - For each qubit i , decide the Pauli operator $Q[i]$ on it by sampling a Pauli operator P from $\beta_i^{k'}$ and setting $Q[i]$ to P .
 - Output Q as the Pauli measurement to carry out.
-

C-LBCS has more parameters and stronger representation power than LBCS. Moreover, the representation power of a C-LBCS scheme can be adjusted by the number of sub-schemes. In the extreme case when there is only one sub-scheme, C-LBCS will degenerate to the original LBCS.

C-LBCS differs from previous methods by providing a *top-down* approach to improve the measurement efficiency, whereas most of the previous methods use the *bottom-up* approach. Previous methods usually solve the problem by considering how to improve a certain measurement scheme (the *bottom*) by certain heuristics. For example, in grouping methods, the scheme is usually l_1 sampling and commuting relations are leveraged to improve it. In the Derand method [22], one improves the distribution from the classical shadow by greedily optimizing a cost function. These methods usually do not involve the concept of an optimal scheme in their derivation since there is no direct way to involve it in its heuristics. However, in C-LBCS, we can directly consider how to approximate an optimal simple scheme (the *top*) and provide heuristics in a top-down manner.

In the following, we show that C-LBCS is capable of representing any distribution of Pauli measurements that are applied to the whole system.

Theorem 1 (Universality of C-LBCS). *Suppose there are n_q qubits in a system. When there are 3^{n_q} sub-schemes, a C-LBCS can simulate any distribution of Pauli measurements if every Pauli measurement Q_k in the distribution acts non-trivially on every qubit.*

Proof. Denote the set of Pauli measurements in the distribution and their probability to be simulated by \vec{Q} and \vec{p} . To simulate this distribution, one just needs to set sub-scheme S_k in the C-LBCS scheme to output Q_k and set $\vec{r} = \vec{p}$. Notice that there are at most 3^{n_q} different Pauli measurements that act on every qubit in the system. Therefore, at most 3^{n_q} sub-schemes are needed. \square

Though C-LBCS might need exponentially many sub-schemes to simulate the optimal simple scheme, in Sec. IV A, we show that state-of-the-art efficiency can be provided by C-LBCS with as many sub-schemes as groups in the OGM method. This implies the number of sub-schemes we need to achieve good efficiency can be far less than exponentially large. In practice, one can adjust the number of sub-schemes by the available computational resources and the required efficiency.

III. OPTIMIZATION OF CMS

One problem with CMS is how to determine the probability of each sub-scheme and calculate its optimal parameters. In the following, we discuss how to optimize CMS, including both the parameters of the sub-schemes and their probabilities, with the assumption that all the measurements involved are Pauli measurements and the state to be measured is totally unknown. We introduce a cost function which has a simple physical interpretation and can be constructed without the knowledge of the target quantum states. Then, we analyze the structure of the cost function and investigate how to perform gradient descent with it.

A. Average one-shot variance

A straightforward way to quantify the performance of a measurement method is using the variance of the estimation it produces, given a fixed number of shots. However, as we mentioned, a post-processing protocol must be specified for measurement schemes producing estimations. In the following, we formalize and adopt a post-processing protocol that is widely adopted [17, 23], in which estimations of terms in the observable are generated and summed up to the estimation of the whole observable. This post-processing protocol is different from the one adopted in Ref. [19, 20], in which only estimations to the whole observable are generated and averaged.

We note that throughout this work, we use $\widetilde{\cdot}$ to represent random variables. Suppose there is a list of Pauli measurement $\{Q_k\}$ generated from the measurement scheme and $\{\widetilde{x}_k\}$ are the corresponding results in the form of bitstrings. Also, we define the following relation that characterizes what

Pauli measurements can produce estimations for the expectation value of a Pauli string.

Definition 4 (Qubit-wise covering). *For a Pauli string P and a Pauli measurement represented by the Pauli string Q , we say Q covers P , or equivalently $P \triangleright Q$, when $P[i]$ equals to either $Q[i]$ or identity for all qubit i .*

With the above notations, we present [Protocol 2](#), which is set to be the post-processing protocol for demonstrating all measurement schemes in this work.

Protocol 2: Observable estimation by estimating each term

- For each term P_j in the observable $O = \sum_j a_j P_j$, generate an estimation $\widetilde{\langle P_j \rangle}$ for it by averaging one-shot estimations

$$\widetilde{\langle P_j \rangle} := \frac{1}{m_j} \sum_{k, P_j \triangleright Q_k} \mu(P_j, \tilde{x}_k), \quad (1)$$

where $m_j = \sum_{k, P_j \triangleright Q_k} 1$ is number of available one-shot estimations and

$$\mu(P_j, \tilde{x}_k) = \prod_{i, P_j[i] \neq I} (-1)^{\tilde{x}_k[i]}, \quad (2)$$

is the one-shot estimation generated by each measurement outcome \tilde{x}_k . Here, $\tilde{x}_k[i]$ is used to denote the i -th bit of \tilde{x}_k .

- Output the estimation of $\langle O \rangle$ by summing up the estimations of each term.

$$\widetilde{\langle O \rangle} = \sum_j a_j \widetilde{\langle P_j \rangle}. \quad (3)$$

For a list of Pauli measurements $\{Q_k\}$, the output $\widetilde{\langle O \rangle}$ of [Protocol 2](#) is random due to the random nature of quantum mechanics. The variance of the estimate of $\widetilde{\langle O \rangle}$ can be calculated by (See [Sec. C](#) for derivation)

$$\begin{aligned} \text{Var}(\widetilde{\langle O \rangle}) &= \sum_{j, \ell} a_j a_\ell \text{Cov}(\widetilde{\langle P_j \rangle}, \widetilde{\langle P_\ell \rangle}) \\ &= \sum_{j, \ell} a_j a_\ell \frac{m_{j\ell}}{m_{jj} m_{\ell\ell}} (\langle P_j P_\ell \rangle - \langle P_j \rangle \langle P_\ell \rangle), \end{aligned} \quad (4)$$

where

$$m_{j\ell} := \sum_{k, P_j \triangleright Q_k, P_\ell \triangleright Q_k} 1, \quad (5)$$

and $\langle \dots \rangle$ here are the true expectation values that depend on the state measured. m_{jj} equals m_j that we defined above and $m_{j\ell}$ ($j \neq \ell$) is the number measurements that generate a one-shot estimation for both $\langle P_j \rangle$ and $\langle P_\ell \rangle$.

When the measurement scheme is stochastic, $m_{j\ell}$ needs to be modelled as a random variable $\tilde{m}_{j\ell}$ and the variance then

needs to be obtained by applying the law of total variance.

$$\text{Var}(\widetilde{\langle O \rangle}) = \sum_{j, \ell} a_j a_\ell \mathbb{E}[\frac{\tilde{m}_{j\ell}}{\tilde{m}_{jj} \tilde{m}_{\ell\ell}}] (\langle P_j P_\ell \rangle - \langle P_j \rangle \langle P_\ell \rangle), \quad (6)$$

The above equation involves $\langle P_j \rangle$ and $\langle P_j P_\ell \rangle$ which depends on the state that is measured. As we assume the target state is unknown, it cannot be directly used as the cost function. Therefore, we propose to use the variance averaged over the whole Hilbert space with the Haar measure using the following lemma.

Lemma 1. *Suppose there are n_q qubits in the system, then*

$$\int_{\text{Haar}} (\langle P_j P_\ell \rangle - \langle P_j \rangle \langle P_\ell \rangle) d|\psi\rangle = \delta_{j\ell} \frac{2^{n_q}}{2^{n_q} + 1}, \quad (7)$$

where $\delta_{j\ell}$ is the Kronecker delta function.

A proof of the lemma is given in [Sec. B](#). With [Lemma 1](#), we have

$$\mathbb{E}_{|\psi\rangle \sim \text{Haar}} [\text{Var}[\langle \psi | \widetilde{\langle O \rangle} | \psi \rangle]] = \sum_j a_j^2 \mathbb{E}[\frac{1}{\tilde{m}_j}] \frac{2^{n_q}}{2^{n_q} + 1}, \quad (8)$$

which is independent of the state to be measured. We remark that we can also show that the variance of the variance $\text{Var}(\widetilde{\langle O \rangle})$ over the whole Hilbert space with the Haar measure is exponentially suppressed (see Section 4 in [\[24\]](#)). Therefore, $\text{Var}(\widetilde{\langle O \rangle})$ tends to take the average value [Eq. \(8\)](#) when sampling $|\psi\rangle$ according to the Haar measure.

Notice that $\mathbb{E}[\frac{1}{\tilde{m}_j}]$ in the right-hand side of [Eq. \(8\)](#) is ill-defined when the probability that \tilde{m}_j equals 0 is non-zero, which is usual when M is finite. To make a well-defined quantifier, we define the ratio between $\mathbb{E}_{|\psi\rangle \sim \text{Haar}} [\text{Var}[\langle \psi | \widetilde{\langle O \rangle} | \psi \rangle]]$ and $1/M$ in the limit that $M \rightarrow +\infty$:

$$V = \lim_{M \rightarrow +\infty} \sum_j a_j^2 \mathbb{E}[\frac{M}{\tilde{m}_j + \epsilon}] \frac{2^{n_q}}{2^{n_q} + 1}, \quad (9)$$

in which the random variable $\frac{M}{\tilde{m}_j + \epsilon}$ will converge to $\frac{M}{\tilde{m}_j}$ when $M \rightarrow +\infty$ if we set $\epsilon \in o(M)$. In the [Sec. D](#), we show that if ϵ is a positive number in $\Theta(M^{\frac{5}{6}})$ and \tilde{m}_j is a well-behaved random variable whose expectation value and variance are both in $\Theta(M)$, we have

$$\lim_{M \rightarrow +\infty} \mathbb{E}[\frac{M}{\tilde{m}_j + \epsilon}] = \lim_{M \rightarrow +\infty} \frac{M}{\mathbb{E}[\tilde{m}_j]} = \frac{1}{h_j}, \quad (10)$$

where h_j can be interpreted as the average probability for the term P_j being covered by a measurement generated by the scheme. As long as $h_j > 0$ for all j , V is well-defined as expected. This formula holds for all simple measurement schemes, since in that case, \tilde{m}_j obeys the binomial distribution whose expectation value and variance grow linearly with M (therefore in $\Theta(M)$). Therefore, in the following, we can reasonably define the cost function we use in this work.

Definition 5 (Average one-shot variance). Suppose there is a n_q qubit observable $O = \sum_j a_j P_j$ and a simple measurement scheme S . The average one-shot variance V of S for O is

$$V = \sum_j \frac{a_j^2}{h_j} \frac{2^{n_q}}{2^{n_q} + 1}, \quad (11)$$

where $h_j = \lim_{M \rightarrow \infty} \mathbb{E}[\tilde{m}_j]/M$.

The physical meaning of V is the scaling factor of the variance of $\langle O \rangle$ averaged by Haar measure in the limit as the number of measurements tends to infinity. A scheme can be optimized by this cost function as long as \tilde{h} can be efficiently estimated given the parameters of the scheme. Notably, the structure of SampleProd allows a further decomposition of \tilde{h} by the contribution of each sub-scheme. Define $\tilde{m}_j^k(M_k)$ to be the number of measurements that cover P_j generated by the sub-scheme S_k with M_k measurements assigned to it. Denote $h_j^k = \lim_{M_k \rightarrow \infty} \mathbb{E}[\tilde{m}_j^k(M_k)]/M_k$. h_j can be decomposed as

$$h_j = \lim_{M \rightarrow \infty} \sum_k \mathbb{E}[\tilde{m}_j^k(M_k)]/M \quad (12)$$

$$= \sum_k \lim_{M \rightarrow \infty} (\mathbb{E}[\tilde{m}_j^k(M_k)]/M_k)(M_k/M) \quad (13)$$

$$= \sum_k r_k h_j^k, \quad (14)$$

where we used that $\lim_{M \rightarrow \infty} M_k/M = r_k$. In this way, V can be rewritten as

$$V = \frac{2^{n_q}}{2^{n_q} + 1} \sum_j \frac{a_j^2}{\sum_k r_k h_j^k}, \quad (15)$$

which will be adopted in all the following sections. In the case of C-LBCS, h_j^k is simply the probability that P_j is covered by the sampled measurement when the k -th LBCS scheme has been sampled. We put the detail of its calculation in Sec. A.

B. Optimization strategy

After setting the cost function, we discuss how to efficiently optimize a CMS made by SampleProd. In V , there are two sets of parameters to be optimized, the probabilities \vec{r} and the parameters $\{\theta_i^k\}$ for each sub-scheme. Here, θ_i^k denotes the i -th parameter for the sub-scheme S_k .

1. Gradient rescale

A straightforward way to optimize \vec{r} and $\{\theta_i^k\}$ is to apply a gradient descent directly. To this end, we calculate the gradient on the parameter θ_i^k as

$$\frac{\partial V}{\partial \theta_i^k} = \sum_j \frac{\partial V}{\partial h_j} \frac{\partial \sum_k r_k h_j^k}{\partial \theta_i^k} = \sum_j \frac{\partial V}{\partial h_j} r_k \frac{\partial h_j^k}{\partial \theta_i^k}. \quad (16)$$

The gradient on θ_i^k can be very small when r_k is close to zero, which may happen when parameters in S_k are poorly initialized and r_k is optimized to nearly zero for avoiding S_k being sampled. In this way, S_k will be frozen out from the composite scheme as its parameters stop updating and its probability to be sampled is nearly zero. This situation should be avoided as we want to utilize all sub-schemes. Thus, we adopt a strategy to rescale the gradient by $1/r_k$ when optimizing the parameters of S_k . Specifically, we use

$$\frac{1}{r_k} \frac{\partial V}{\partial \theta_i^k} = \sum_j \frac{\partial V}{\partial h_j} \frac{\partial h_j^k}{\partial \theta_i^k}. \quad (17)$$

instead of Eq. (16) in the gradient descent. The rescaled gradient ensures that each sub-scheme continues to be optimized even if their r_k is small.

2. Two time-scale update rule

As the second technique, we introduce the two time-scale update rule (TTUR) [21], in which the parameters of the model are divided into two parts and optimized with different learning rates. Before going into detail, we clarify the feature of the cost function Eq. (15) in terms of convexity. As the term $r_k h_j^k$ is included, the cost function Eq. (15) is non-convex, and the optimization may be trapped in a local minimum. However, we show that the cost function V is convex as a function of \vec{r} (with $\{\theta_i^k\}$ and therefore $\{h_j^k\}$ fixed) or $\{h_j^k\}$ (with \vec{r} fixed).

Let us first prove the convexity with respect to $\{h_j^k\}$ when \vec{r} is fixed. The same proof can be used to show the convexity of V when $\{\vec{h}_j^k\}$ is fixed. Recall that a summation of convex functions weighted by positive numbers is also a convex function. Since V is a summation of the terms $\{1/(\sum_k r_k h_j^k)\}$ weighted by positive numbers, we just need to prove the convexity of each term. Then, notice that $1/(\sum_k r_k h_j^k)$ is just a composition of $f(x) = 1/x$ and $g_j(\{h_j^k\}) = \sum_k r_k h_j^k$. Because g_j is concave and positive on its domain, combined with the fact that $f(x)$ is convex and non-increasing when $x > 0$, we know that $f(g_j(\{h_j^k\})) = 1/(\sum_k r_k h_j^k)$ is convex. Since $\{h_j^k\}$ is defined on a convex set ($h_j^k \in [0, 1]$), combined with the above arguments, we see V is a convex function of $\{\vec{h}_j^k\}$ when \vec{r} is fixed.

The structure that V is convex when \vec{r} or $\{h_j^k\}$ is fixed implies the optimization will be easier when only \vec{r} or $\{h_j^k\}$ (or $\{\theta_i^k\}$) is optimized. This situation is similar to the training of a generative adversarial network (GAN) [25], in which the training can also be divided into two parts (the generator and the discriminator), whose optimization is easier with the parameters of the other part fixed. Therefore, we propose to adopt the same strategy in the optimization of the probabilities \vec{r} and parameters in the sub-schemes and set different learning rates for \vec{r} and $\{\theta_i^k\}$ when optimizing a CMS. Throughout this work, we will set the learning rate of \vec{r} to be 10 times smaller than the learning rate of $\{\theta_i^k\}$.

3. Stochastic gradient descent

Stochastic gradient descent (SGD) is a widely adopted strategy in machine learning, in which the gradient provided to the optimizer is generated only with part of the whole dataset. SGD provides a general approach for training models when the dataset is large. In our case, the models (measurement schemes) are trained with the terms from the observable. An observable might contain a large number of terms in near-term quantum algorithms. For electronic structure problems (the main target of VQE), the number of terms in the Hamiltonian contains $\mathcal{O}(n_O^4)$ terms [26], with n_O being the number of spin-orbitals. If the Hamiltonian is not split, it will be hard to fit the computation in the memory of a GPU.

Therefore, we propose to use SGD in the training of measurement schemes. Specifically, in each epoch, we randomly split the terms of observable O into batches $\{O_j\}$, with each of them containing a nearly fixed number of terms and $\sum_j O_j = O$. Then, we iterate over $\{O_j\}$ and calculate the gradient in each step with one batch. After iterating all the batches, we split O with a different seed for the next epoch. We show in Sec. IV B that C-LBCS can perform well even when the batch size is very small.

IV. NUMERICAL EXAMPLES FOR C-LBCS

In the following, we numerically demonstrate the performance of C-LBCS with the average one-shot variance as the quantifier. In C-LBCS, the number of sub-schemes affects the performance of the composite scheme. We show that a C-LBCS can outperform previous state-of-the-art methods by using a proper number of sub-schemes. We also analyze how different training strategies can affect the convergence of optimization.

Throughout this section, by default, both the Rescale and TTUR strategies are adopted in the training. All probabilities (\vec{r} and $\{\beta_i^k\}$) are calculated by passing parameters into SoftPlus and normalization layers (See Sec. E). The batch size for stochastic gradient descent is set to 500 Pauli strings and the learning rate for all optimizations is 5×10^{-3} for sub-scheme parameters and 5×10^{-4} for \vec{r} . Optimizations terminate when the cost function fails to decrease more than 0.1% in the past 1000 steps. The initial parameters for the LBCS schemes are set so that the C-LBCS scheme resembles the l_1 sampling scheme. For a C-LBCS scheme with n_S sub-schemes, we select the n_S terms with the largest weights ($|a_j|$) in O and set the LBCS sub-schemes to generate them initially. The probabilities \vec{r} of each sub-scheme are set to be proportional to the weight of those terms correspondingly.

The molecular Hamiltonians are generated by mapping the Fermionic Hamiltonian for the electronic structure problem with Jordan-Wigner (JW) [27] and Bravyi-Kitaev (BK) [28] transformations. All molecules are in their equilibrium geometry and under the STO-3G basis set, except for hydrogen chains, in which the hydrogens are spaced by 2 Bohr radius and the STO-6G basis set is used. The equilibrium geometries are retrieved from [29].

A. Performance

We test our method by comparing its performance on molecular Hamiltonians against previous methods, including the derandomized classical shadow (Derand) [22], OGM and ShadowGrouping (SG) [30]. The number of sub-schemes of C-LBCS is set to be the same as the number of groups generated in OGM. Since the average one-shot variance is defined in the limit of infinitely many measurements, it is hard to estimate it in the exact same way for Derand and SG because the $\{h_j\}$ in these methods cannot be analytically calculated. Here, for a Hamiltonian with n_H terms, we choose to generate $3n_H$ measurements for each method and calculate the average one-shot variance by the measurement scheme that uniformly samples the $3n_H$ measurements. We note that $3n_H$ is a number much larger than that used in the original works of Derand and SG (1000 shots). Some of the exact numbers of n_H are shown in Table III.

The result of experiments is shown in Table I. We see that in all cases except for H_2O molecule with BK transformation, C-LBCS outperforms previous methods, which confirms the validity of the composite measurement schemes. Our results agree with the results of the work of SG, though they are not using average one-shot variance as the metrics.

Molecule	Enc.	Derand	OGM	SG	C-LBCS
LiH(12)	JW	8.26	7.62	6.85	6.53
	BK	10.68	7.85	7.16	6.77
$H_6(12)$	JW	32.64	30.47	27.35	24.93
	BK	48.25	35.91	35.21	30.68
$H_2O(14)$	JW	712	479	432	430
	BK	891	518	454	455
$NH_3(16)$	JW	833	357	289	287
	BK	1111	399	312	309
$N_2(20)$	JW	1571	1115	827	811
	BK	2002	1045	852	841
$C_2H_2(24)$	JW	1708	880	638	580
	BK	2424	879	645	614
$C_2H_4(28)$	JW	3692	1481	1004	928
	BK	4908	1641	1040	1018
$CO_2(30)$	JW	11655	3500	2442	2335
	BK	16349	4169	2754	2677

TABLE I. Table for the average one-shot variance with various measurement methods. C-LBCS with a moderate number of sub-schemes outperforms the other methods in nearly all the systems.

We also study how the average one-shot variance of C-LBCS changes with the number of sub-schemes. The results are shown in Fig. 2, with SG as a reference of variance (red line) and OGM as a reference of the number of sub-schemes (yellow line). We found that C-LBCS constantly outperforms SG with a number of sub-schemes comparable to the number of OGM groups. Fig. 2 also implies that better measurement efficiency can be obtained by increasing the number of sub-schemes. This property of C-LBCS distinguishes it from many previous methods, in which no hyperparameters can be used to trade measurement efficiency with computational resources.

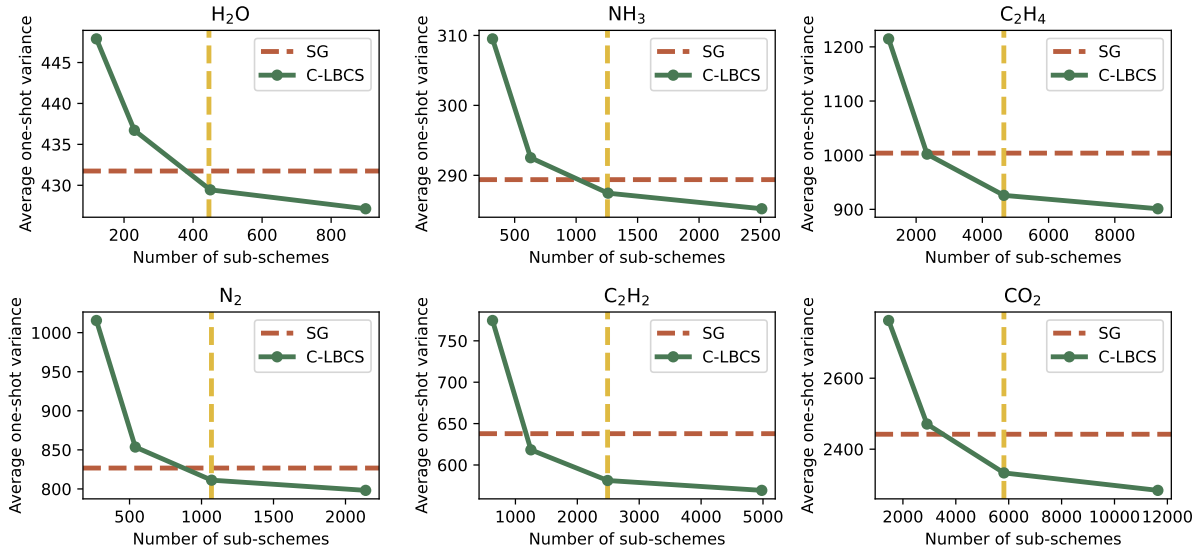


FIG. 2. The performance of C-LBCS with different numbers of sub-schemes, quantified by the average one-shot variance. All the Hamiltonians are encoded by JW transformation. The vertical yellow line represents the number of groups produced by the OGM method. The horizontal red line represents the average one-shot variance of the ShadowGrouping method.

B. Training

We numerically study how different strategies for parameter optimization affects the convergence of training. We do ablation tests in which *Rescale* or *TTUR* is turned off during training. Other settings of the training are kept the same as adopted by Table I. All Hamiltonians are encoded with the JW transformation and the result is shown in Table II. We find that keeping both of the strategies provide the best result in most cases.

Molecule	None	Rescale	TTUR	Both
N ₂ (20)	825	807	815	811
C ₂ H ₂ (24)	606	592	586	580
C ₂ H ₄ (28)	977	945	935	928
CO ₂ (30)	2379	2335	2346	2335
H ₆ (12)	25.67	25.35	25.59	24.93
H ₈ (16)	91.52	88.76	83.71	83.54
H ₁₀ (20)	251	229	222	219
H ₁₂ (24)	581	521	501	496

TABLE II. The average one-shot variance by C-LBCS with different strategies in optimization. We find that applying the *Rescale* and *TTUR* strategies can significantly improve the result of training. In most cases, applying both of these strategies provides the best result and in a few cases applying *Rescale* alone gives the best result.

We then study how different batch sizes affect the training of C-LBCS. We set the batch sizes n_b to be $1/128$, $1/64$ and $1/32$ of the number of terms in the Hamiltonian n_H . To make a fair comparison, we adjust the stop criteria proportionally, so that the optimization terminates when the cost function fails to decrease more than 0.1% in the past $1000 \times \frac{500}{n_b}$ steps. The Hamiltonians are encoded with the BK transformation. We

show in Table III that the cost function converges to similar values, which implies the training of C-LBCS is not sensitive to batch size for molecular Hamiltonians. Our result indicates that C-LBCS can be applied on much larger molecular Hamiltonians and trained efficiently on GPUs.

Molecule	n_H	$1/128$	$1/64$	$1/32$
H ₂ O(14)	1085	452.73	454.39	454.85
NH ₃ (16)	2936	307.15	307.44	307.56
N ₂ (20)	2238	837.86	838.31	839.16
C ₂ H ₂ (24)	5184	611.07	610.78	611.42
C ₂ H ₄ (28)	8918	1014.12	1013.51	1014.39
CO ₂ (30)	11433	2663.98	2666.21	2678.22

TABLE III. The average one-shot variance by C-LBCS with batch sizes to be $1/128$, $1/64$ and $1/32$ of the number of terms in the Hamiltonian (n_H). It can be seen that the batch size does not significantly affect the training result of C-LBCS.

V. DISCUSSION & OUTLOOK

In this work, we proposed a new approach, the composite measurement scheme, to combine multiple measurement schemes and explored a new and scalable path for improving the efficiency of observable estimation. As an example of the CMS, based on the SampleProd operator, we found an easily trainable composite measurement scheme C-LBCS and numerically showed how C-LBCS can outperform previous state-of-the-art methods. We studied the trainability of C-LBCS, proposed to rescale the gradients for optimization and revealed a two-level structure in the cost function. We also found that C-LBCS can be trainable by stochastic gradi-

ent descent with small batch sizes, so the model will be trainable with much larger observables.

We used the average one-shot variance as our cost function and performance quantifier, which does not involve any information about the state to be measured. This is different from many previous works [16, 20, 30] which use the variance concerning a certain state (e.g. the ground state of the Hamiltonian) as the performance quantifier. We chose not to follow this approach because we do not expect the ground state (or its approximation) to be always available, especially when 40 or more qubits are involved. For the same reason, we also adopted a cost function that does not involve the information from a pre-calculated state. However, in practice, it might be advantageous to use the information of states collected from measurement results to improve the estimation efficiency [23]. We leave improving C-LBCS this way as a future question to be investigated.

For more generalization of this work, as we only demonstrated one type of composite measurement scheme, it will be interesting to see whether better measurement schemes can be produced by applying SampleProd on other types of subschemes with more complex structure [31, 32]. Also, as we assumed that only Pauli measurements are allowed considering the implementation hardness, it will be interesting to see how our framework can be generalized to more types of measurements, such as Clifford measurements.

ACKNOWLEDGMENTS

The authors thank Anders G. Frøseth for his generous support. K.N. acknowledges the support of Grant-in-Aid for JSPS Research Fellow 22J01501. A.A.-G. also acknowledges the generous support of Natural Resources Canada and the Canada 150 Research Chairs program.

-
- [1] Frank Arute, Kunal Arya, Ryan Babbush, Dave Bacon, Joseph C Bardin, Rami Barends, Rupak Biswas, Sergio Boixo, Fernando GSL Brandao, David A Buell, *et al.*, “Quantum supremacy using a programmable superconducting processor,” *Nature* **574**, 505–510 (2019).
 - [2] Han-Sen Zhong, Hui Wang, Yu-Hao Deng, Ming-Cheng Chen, Li-Chao Peng, Yi-Han Luo, Jian Qin, Dian Wu, Xing Ding, Yi Hu, *et al.*, “Quantum computational advantage using photons,” *Science* **370**, 1460–1463 (2020).
 - [3] Lars S Madsen, Fabian Laudenbach, Mohsen Falamarzi Askarani, Fabien Rortais, Trevor Vincent, Jacob FF Bulmer, Filippo M Miatto, Leonhard Neuhaus, Lukas G Helt, Matthew J Collins, *et al.*, “Quantum computational advantage with a programmable photonic processor,” *Nature* **606**, 75–81 (2022).
 - [4] John Preskill, “Quantum computing in the nisy era and beyond,” *Quantum* **2**, 79 (2018).
 - [5] Kishor Bharti, Alba Cervera-Lierta, Thi Ha Kyaw, Tobias Haug, Sumner Alperin-Lea, Abhinav Anand, Matthias Degroote, Hermann Heimonen, Jakob S Kottmann, Tim Menke, *et al.*, “Noisy intermediate-scale quantum algorithms,” *Reviews of Modern Physics* **94**, 015004 (2022).
 - [6] Marco Cerezo, Andrew Arrasmith, Ryan Babbush, Simon C Benjamin, Suguru Endo, Keisuke Fujii, Jarrod R McClean, Kosuke Mitarai, Xiao Yuan, Lukasz Cincio, *et al.*, “Variational quantum algorithms,” *Nature Reviews Physics* **3**, 625–644 (2021).
 - [7] Alberto Peruzzo, Jarrod McClean, Peter Shadbolt, Man-Hong Yung, Xiao-Qi Zhou, Peter J Love, Alán Aspuru-Guzik, and Jeremy L O’Brien, “A variational eigenvalue solver on a photonic quantum processor,” *Nature comm.* **5**, 4213 (2014).
 - [8] Ying Li and Simon C Benjamin, “Efficient variational quantum simulator incorporating active error minimization,” *Physical Review X* **7**, 021050 (2017).
 - [9] Nicholas H Stair, Renke Huang, and Francesco A Evangelista, “A multireference quantum krylov algorithm for strongly correlated electrons,” *Journal of Chemical Theory and Computation* **16**, 2236–2245 (2020).
 - [10] Harper R Grimsley, Sophia E Economou, Edwin Barnes, and Nicholas J Mayhall, “An adaptive variational algorithm for exact molecular simulations on a quantum computer,” *Nature comm.* **10**, 1–9 (2019).
 - [11] Zi-Jian Zhang, Jinzhao Sun, Xiao Yuan, and Man-Hong Yung, “Low-depth hamiltonian simulation by an adaptive product formula,” *Physical Review Letters* **130**, 040601 (2023).
 - [12] Suguru Endo, Zhenyu Cai, Simon C. Benjamin, and Xiao Yuan, “Hybrid quantum-classical algorithms and quantum error mitigation,” *Journal of the Physical Society of Japan* **90**, 032001 (2021), <https://doi.org/10.7566/JPSJ.90.032001>.
 - [13] William J. Huggins, Sam McArdle, Thomas E. O’Brien, Joonho Lee, Nicholas C. Rubin, Sergio Boixo, K. Birgitta Whaley, Ryan Babbush, and Jarrod R. McClean, “Virtual distillation for quantum error mitigation,” *Phys. Rev. X* **11**, 041036 (2021).
 - [14] Jinzhao Sun, Xiao Yuan, Takahiro Tsunoda, Vlatko Vedral, Simon C. Benjamin, and Suguru Endo, “Mitigating realistic noise in practical noisy intermediate-scale quantum devices,” (2020), [arXiv:2001.04891 \[quant-ph\]](https://arxiv.org/abs/2001.04891).
 - [15] Vladyslav Verteletskyi, Tzu-Ching Yen, and Artur F Izmaylov, “Measurement optimization in the variational quantum eigensolver using a minimum clique cover,” *The Journal of chemical physics* **152**, 124114 (2020).
 - [16] Bujiao Wu, Jinzhao Sun, Qi Huang, and Xiao Yuan, “Overlapped grouping measurement: A unified framework for measuring quantum states,” *Quantum* **7**, 896 (2023).
 - [17] Tzu-Ching Yen, Aadithya Ganeshram, and Artur F Izmaylov, “Deterministic improvements of quantum measurements with grouping of compatible operators, non-local transformations, and covariance estimates,” *npj Quantum Information* **9**, 14 (2023).
 - [18] Seonghoon Choi, Tzu-Ching Yen, and Artur F Izmaylov, “Improving quantum measurements by introducing “ghost” pauli products,” *Journal of Chemical Theory and Computation* **18**, 7394–7402 (2022).
 - [19] Hsin-Yuan Huang, Richard Kueng, and John Preskill, “Predicting many properties of a quantum system from very few measurements,” *Nature Physics* **16**, 1050–1057 (2020).
 - [20] Charles Hadfield, Sergey Bravyi, Rudy Raymond, and Antonio Mezzacapo, “Measurements of quantum hamiltonians with locally-biased classical shadows,” *Communications in Mathematical Physics* **391**, 951–967 (2022).
 - [21] Martin Heusel, Hubert Ramsauer, Thomas Unterthiner, Bern-

- hard Nessler, and Sepp Hochreiter, “Gans trained by a two time-scale update rule converge to a local nash equilibrium,” *Advances in neural information processing systems* **30** (2017).
- [22] Hsin-Yuan Huang, Richard Kueng, and John Preskill, “Efficient estimation of pauli observables by derandomization,” *Phys. Rev. Lett.* **127**, 030503 (2021).
- [23] Ariel Shlosberg, Andrew J Jena, Priyanka Mukhopadhyay, Jan F Haase, Felix Leditzky, and Luca Dellantonio, “Adaptive estimation of quantum observables,” *Quantum* **7**, 906 (2023).
- [24] Kouhei Nakaji, Suguru Endo, Yuichiro Matsuzaki, and Hideaki Hakoshima, “Measurement optimization of variational quantum simulation by classical shadow and derandomization,” arXiv preprint arXiv:2208.13934 (2022).
- [25] Ian Goodfellow, Jean Pouget-Abadie, Mehdi Mirza, Bing Xu, David Warde-Farley, Sherjil Ozair, Aaron Courville, and Yoshua Bengio, “Generative adversarial networks,” *Commun. ACM* **63**, 139–144 (2020).
- [26] Sam McArdle, Suguru Endo, Alán Aspuru-Guzik, Simon C. Benjamin, and Xiao Yuan, “Quantum computational chemistry,” *Rev. Mod. Phys.* **92**, 015003 (2020).
- [27] Eugene P Wigner and Pascual Jordan, “Über das paulische äquivalenzverbot,” *Z. Phys* **47**, 631 (1928).
- [28] Sergey B Bravyi and Alexei Yu Kitaev, “Fermionic quantum computation,” *Ann. Phys.* **298**, 210–226 (2002).
- [29] Russell D Johnson *et al.*, “Nist computational chemistry comparison and benchmark database,” *NIST Standard Reference Database Number 101* (2022), 10.18434/T47C7Z.
- [30] Alexander Gresch and Martin Kliesch, “Guaranteed efficient energy estimation of quantum many-body hamiltonians using shadowgrouping,” arXiv preprint arXiv:2301.03385 (2023).
- [31] Stefan Hillmich, Charles Hadfield, Rudy Raymond, Antonio Mezzacapo, and Robert Wille, “Decision diagrams for quantum measurements with shallow circuits,” in *2021 IEEE International Conference on Quantum Computing and Engineering (QCE)* (IEEE, 2021) pp. 24–34.
- [32] Ahmed A Akhtar, Hong-Ye Hu, and Yi-Zhuang You, “Scalable and flexible classical shadow tomography with tensor networks,” arXiv preprint arXiv:2209.02093 (2022).
- [33] Benoît Collins and Piotr Śniady, “Integration with respect to the Haar measure on unitary, orthogonal and symplectic group,” *Communications in Mathematical Physics* **264**, 773–795 (2006).
- [34] Adam Paszke, Sam Gross, Francisco Massa, Adam Lerer, James Bradbury, Gregory Chanan, Trevor Killeen, Zeming Lin, Natalia Gimelshein, Luca Antiga, *et al.*, “Pytorch: An imperative style, high-performance deep learning library,” *Advances in neural information processing systems* **32** (2019).

Appendix A: Evaluation of average one-shot variance for C-LBCS

In this section, we provide the formula for calculating $\{h_j^k\}$ for C-LBCS schemes, so that the average one-shot variance of it can be calculated by Eq. (15).

Notice that when a LBCS scheme samples a Pauli string, the sampling of the Pauli operator on each qubit is independent of each other. Therefore, we can simply use the multiplication rule to calculate the probability. Denote the Pauli operator on the i -th qubit in the Pauli string P_j by $P_j[i]$ and denote the probability that Pauli operator P is sampled from the distribution β_i^k by $\beta_i^k(P)$, we have

$$h_j^k = \prod_{i=1}^{n_q} p(P_j[i], \beta_i^k), \quad (\text{A1})$$

where we define

$$p(P_j[i], \beta_i^k) = \begin{cases} \beta_i^k(P_j[i]), & P_j[i] \in \{X, Y, Z\} \\ 1, & P_j[i] = I \end{cases}. \quad (\text{A2})$$

Appendix B: Proof of Lemma 1

With $|\bar{0}\rangle = |0\rangle^{\otimes n_q}$, it holds

$$\int_{\text{Haar}} (\langle P_j P_\ell \rangle - \langle P_j \rangle \langle P_\ell \rangle) d|\psi\rangle = \int_{\text{Haar}} dU (\langle \bar{0} | U^\dagger P_j P_\ell U | \bar{0} \rangle - \langle \bar{0} | U^\dagger P_j U | \bar{0} \rangle \langle \bar{0} | U^\dagger P_\ell U | \bar{0} \rangle). \quad (\text{B1})$$

For calculating the average over the whole Hilbert space with Haar measure, we use the element-wise integration formula [33]:

$$\int_{\text{Haar}} dU U_{a_1 b_1} U_{a'_1 b'_1}^* = \frac{1}{N} \delta_{a_1 a'_1} \delta_{b_1 b'_1}, \quad (\text{B2})$$

$$\int_{\text{Haar}} dU U_{a_1 b_1} U_{a_2 b_2} U_{a'_1 b'_1}^* U_{a'_2 b'_2}^* = \frac{\delta_{a_1 a'_1} \delta_{a_2 a'_2} \delta_{b_1 b'_1} \delta_{b_2 b'_2} + \delta_{a_1 a'_2} \delta_{a_2 a'_1} \delta_{b_1 b'_2} \delta_{b_2 b'_1}}{N^2 - 1} - \frac{\delta_{a_1 a'_1} \delta_{a_2 a'_2} \delta_{b_1 b'_2} \delta_{b_2 b'_1} + \delta_{a_1 a'_2} \delta_{a_2 a'_1} \delta_{b_1 b'_1} \delta_{b_2 b'_2}}{N(N^2 - 1)}, \quad (\text{B3})$$

with N as the dimension of the Hilbert space of U . For the first term in Eq. (B1), it holds

$$\begin{aligned} \int_{\text{Haar}} dU \langle \bar{0} | U^\dagger P_j P_\ell U | \bar{0} \rangle &= \sum_{a,b} U_{a0}^* [P_j P_\ell]_{ab} U_{b0} \\ &= \frac{1}{2^{n_q}} \text{Tr}(P_j P_\ell), \end{aligned} \quad (\text{B4})$$

where we denote (a, b) element of $P_j P_\ell$ as $[P_j P_\ell]_{ab}$, and we used Eq. (B2) in the second equality. For the second term in Eq. (B1), it holds

$$\begin{aligned} \int_{\text{Haar}} dU \langle \bar{0} | U^\dagger P_j U | \bar{0} \rangle \langle \bar{0} | U^\dagger P_\ell U | \bar{0} \rangle &= \sum_{a,b,c,d} U_{a0}^* [P_j]_{ab} U_{b0} U_{c0}^* [P_\ell]_{cd} U_{d0} \\ &= \frac{1}{2^{2n_q} - 1} \sum_{a,b,c,d} [P_j]_{ab} [P_\ell]_{cd} \left(\delta_{ba} \delta_{dc} + \delta_{bc} \delta_{da} - \frac{1}{2^{n_q}} (\delta_{ba} \delta_{dc} + \delta_{bc} \delta_{da}) \right) \\ &= \frac{1}{2^{2n_q} - 1} \left(1 - \frac{1}{2^{n_q}} \right) (\text{Tr}(P_j) \text{Tr}(P_\ell) + \text{Tr}(P_j P_\ell)) \\ &= \frac{1}{2^{n_q} (2^{n_q} + 1)} (\text{Tr}(P_j) \text{Tr}(P_\ell) + \text{Tr}(P_j P_\ell)), \end{aligned} \quad (\text{B5})$$

where in the second equality, we use Eq. (B3). Finally, substituting Eq. (B4) and Eq. (B5) into Eq. (B1), we obtain

$$\begin{aligned} \int_{\text{Haar}} (\langle P_j P_\ell \rangle - \langle P_j \rangle \langle P_\ell \rangle) d|\psi\rangle &= \frac{1}{2^{n_q}} \text{Tr}(P_j P_\ell) - \frac{1}{2^{n_q} (2^{n_q} + 1)} (\text{Tr}(P_j) \text{Tr}(P_\ell) + \text{Tr}(P_j P_\ell)) \\ &= \delta_{j\ell} \frac{2^{n_q}}{2^{n_q} + 1}, \end{aligned} \quad (\text{B6})$$

where in the second equality, we used

$$\text{Tr}(P_j P_\ell) = 2^{n_q} \delta_{j\ell}, \quad \text{Tr}(P_j) = 0, \quad (\text{B7})$$

which holds since $P_j, P_\ell \in \{X, Y, Z, I\}^{\otimes n_q}$ and $P_j, P_\ell \neq I^{\otimes n_q}$ with X, Y, Z being Pauli operators and I being the identity operator.

Appendix C: Derivation of Eq. (4)

To prove

$$\text{Var}(\langle \widetilde{O} \rangle) = \sum_{j,\ell} a_j a_\ell \text{Cov}(\langle \widetilde{P_j} \rangle, \langle \widetilde{P_\ell} \rangle) = \sum_{j,\ell} a_j a_\ell \frac{m_{j\ell}}{m_{jj} m_{\ell\ell}} (\langle P_j P_\ell \rangle - \langle P_j \rangle \langle P_\ell \rangle), \quad (\text{C1})$$

It will suffice by showing

$$\text{Cov}(\langle \widetilde{P_j} \rangle, \langle \widetilde{P_\ell} \rangle) = \frac{m_{j\ell}}{m_{jj} m_{\ell\ell}} (\langle P_j P_\ell \rangle - \langle P_j \rangle \langle P_\ell \rangle). \quad (\text{C2})$$

Recall that $\langle \widetilde{P_j} \rangle$ and $\langle \widetilde{P_\ell} \rangle$ can be decomposed into the summation

$$\langle \widetilde{P_j} \rangle := \frac{1}{m_{jj}} \sum_{k, P_j \triangleright Q_k} \mu(P_j, \tilde{x}_k), \quad (\text{C3})$$

which can be substituted into the expression of covariance and yields

$$\text{Cov}(\langle \widetilde{P_j} \rangle, \langle \widetilde{P_\ell} \rangle) \quad (\text{C4})$$

$$= \text{Cov}\left(\frac{1}{m_{jj}} \sum_{k, P_j \triangleright Q_k} \mu(P_j, \tilde{x}_k), \frac{1}{m_{\ell\ell}} \sum_{k, P_\ell \triangleright Q_k} \mu(P_\ell, \tilde{x}_k)\right) \quad (\text{C5})$$

$$= \frac{1}{m_{jj} m_{\ell\ell}} \text{Cov}\left(\sum_{k, P_j \triangleright Q_k} \mu(P_j, \tilde{x}_k), \sum_{k, P_\ell \triangleright Q_k} \mu(P_\ell, \tilde{x}_k)\right) \quad (\text{C6})$$

$$= \frac{1}{m_{jj} m_{\ell\ell}} \sum_{k_1, P_j \triangleright Q_{k_1}} \sum_{k_2, P_\ell \triangleright Q_{k_2}} \text{Cov}(\mu(P_j, \tilde{x}_{k_1}), \mu(P_\ell, \tilde{x}_{k_2})). \quad (\text{C7})$$

Notice that when $k_1 \neq k_2$, $\mu(\cdot, \tilde{x}_{k_1})$ and $\mu(\cdot, \tilde{x}_{k_2})$ are independent of each other and their covariance $\text{Cov}(\mu(\cdot, \tilde{x}_{k_1}), \mu(\cdot, \tilde{x}_{k_2}))$ is zero. Therefore, The equation can be simplified to

$$\text{Cov}(\langle \widetilde{P_j} \rangle, \langle \widetilde{P_\ell} \rangle) \quad (\text{C8})$$

$$= \frac{1}{m_{jj}m_{\ell\ell}} \sum_{k, P_j \triangleright Q_k, P_\ell \triangleright Q_k} \text{Cov}(\mu(P_j, \tilde{x}_k), \mu(P_\ell, \tilde{x}_k)) \quad (\text{C9})$$

$$= \frac{1}{m_{jj}m_{\ell\ell}} \sum_{k, P_j \triangleright Q_k, P_\ell \triangleright Q_k} \left(\mathbb{E}[\mu(P_j, \tilde{x}_k)\mu(P_\ell, \tilde{x}_k)] - \mathbb{E}[\mu(P_j, \tilde{x}_k)]\mathbb{E}[\mu(P_\ell, \tilde{x}_k)] \right) \quad (\text{C10})$$

$$(\text{C11})$$

By the definition of $\mu(\cdot, \tilde{x}_k)$, it can be deduced that, when $P_j \triangleright Q_k, P_\ell \triangleright Q_k$, $\mathbb{E}[\mu(P_j, \tilde{x}_k)]$ and $\mathbb{E}[\mu(P_\ell, \tilde{x}_k)]$ equal to $\langle P_j \rangle$ and $\langle P_\ell \rangle$ respectively. It can also be derived from the definition that $\mathbb{E}[\mu(P_j, \tilde{x}_k)\mu(P_\ell, \tilde{x}_k)] = \langle P_j P_\ell \rangle$. With the definition $m_{j\ell} = \sum_{k, P_j \triangleright Q_k, P_\ell \triangleright Q_k} 1$, we have the final expression

$$\text{Cov}(\langle \widetilde{P_j} \rangle, \langle \widetilde{P_\ell} \rangle) = \frac{m_{j\ell}}{m_{jj}m_{\ell\ell}} (\langle P_j P_\ell \rangle - \langle P_j \rangle \langle P_\ell \rangle). \quad (\text{C12})$$

Appendix D: Taylor expansion of expectation value

Let us first give the Taylor expansion of $f(x) = \frac{1}{x}$ to the first order with the Lagrange remainder:

$$\frac{1}{x} = \frac{1}{a} - \frac{1}{a^2}(x - a) + \frac{1}{c(x, a)^3}(x - a)^2, \quad (\text{D1})$$

where $c(x, a)$ is a real number in between x and a . Setting a to be $\mathbb{E}[\tilde{m}_j] + \epsilon$ and x to be $\tilde{m}_j + \epsilon$, we have

$$\frac{M}{\tilde{m}_j + \epsilon} = \frac{M}{\mathbb{E}[\tilde{m}_j] + \epsilon} - \frac{M}{(\mathbb{E}[\tilde{m}_j] + \epsilon)^2}(\tilde{m}_j - \mathbb{E}[\tilde{m}_j]) + \frac{M}{c(\tilde{m}_j + \epsilon, \mathbb{E}[\tilde{m}_j] + \epsilon)^3}(\tilde{m}_j - \mathbb{E}[\tilde{m}_j])^2. \quad (\text{D2})$$

Taking expectation value on both sides, we have

$$\mathbb{E}\left[\frac{M}{\tilde{m}_j + \epsilon}\right] = \frac{M}{\mathbb{E}[\tilde{m}_j] + \epsilon} + \frac{M}{c(\tilde{m}_j + \epsilon, \mathbb{E}[\tilde{m}_j] + \epsilon)^3} \text{Var}(\tilde{m}_j). \quad (\text{D3})$$

In the following, we will prove that, if $\mathbb{E}[\tilde{m}_j] \in \Theta(M)$, $\text{Var}(\tilde{m}_j) \in \Theta(M)$ and $\epsilon = \Theta(M^{5/6})$, we have

$$\lim_{M \rightarrow +\infty} \mathbb{E}\left[\frac{M}{\tilde{m}_j + \epsilon}\right] = \lim_{M \rightarrow +\infty} \frac{M}{\mathbb{E}[\tilde{m}_j]}. \quad (\text{D4})$$

These assumptions are satisfied if \tilde{m}_j is a binomial distribution with M experiments. By using $c(\tilde{m}_j + \epsilon, \mathbb{E}[\tilde{m}_j] + \epsilon) \leq M + \epsilon$, we have the lower bound

$$\mathbb{E}\left[\frac{M}{\tilde{m}_j + \epsilon}\right] \geq \frac{M}{\mathbb{E}[\tilde{m}_j] + \epsilon} + \frac{M}{(M + \epsilon)^3} \text{Var}(\tilde{m}_j). \quad (\text{D5})$$

In the limit that $M \rightarrow +\infty$, we have

$$\lim_{M \rightarrow +\infty} \mathbb{E}\left[\frac{M}{\tilde{m}_j + \epsilon}\right] \geq \lim_{M \rightarrow +\infty} \left(\frac{1}{\mathbb{E}[\tilde{m}_j]/M + \Theta(M^{5/6})/M} + \frac{M}{\Theta(M)^3} \Theta(M) \right) = \lim_{M \rightarrow +\infty} \frac{M}{\mathbb{E}[\tilde{m}_j]}. \quad (\text{D6})$$

For the other side, by using $c(\tilde{m}_j + \epsilon, \mathbb{E}[\tilde{m}_j] + \epsilon) \geq \epsilon$, we have

$$\mathbb{E}\left[\frac{M}{\tilde{m}_j + \epsilon}\right] \leq \frac{M}{\mathbb{E}[\tilde{m}_j] + \epsilon} + \frac{M}{\epsilon^3} \text{Var}(\tilde{m}_j). \quad (\text{D7})$$

In the limit that $M \rightarrow +\infty$, we have

$$\lim_{M \rightarrow +\infty} \mathbb{E}\left[\frac{M}{\tilde{m}_j + \epsilon}\right] \leq \lim_{M \rightarrow +\infty} \frac{M}{\mathbb{E}[\tilde{m}_j]} + \lim_{M \rightarrow +\infty} \frac{\Theta(M^2)}{\Theta(M^{5/6})^3} = \lim_{M \rightarrow +\infty} \frac{M}{\mathbb{E}[\tilde{m}_j]}. \quad (\text{D8})$$

Therefore, by bounds from both sides, we can see that

$$\lim_{M \rightarrow +\infty} \mathbb{E}\left[\frac{M}{\tilde{m}_j + \epsilon}\right] = \lim_{M \rightarrow +\infty} \frac{M}{\mathbb{E}[\tilde{m}_j]}. \quad (\text{D9})$$

Appendix E: Detail about training

All the optimizations in this work are done by PyTorch [34] with the Adam optimizer. To parameterize every probability vector \vec{r} , which satisfies $r_i > 0$ and $\sum_i r_i = 1$, we use a vector \vec{y} of real numbers and set $\vec{r} = \text{Normalize}(\text{SoftPlus}(\vec{\theta}))$. Here, SoftPlus is applied element-wise to $\vec{\theta}$ as

$$\text{SoftPlus}(\theta_i) = \frac{1}{\beta} \log(1 + \exp(\beta \times \theta_i)). \quad (\text{E1})$$

Normalize is defined as

$$\text{Normalize}(\vec{z}) = \frac{\vec{z}}{\sum_i z_i}. \quad (\text{E2})$$

Appendix F: Time used for training

We present the running time of training the C-LBCS models for the results in Table I. The training is carried out on one NVIDIA GeForce RTX 2070 graphics card.

Molecule	Enc.	Time used (s)
LiH(12)	JW	14.3
	BK	9.6
H ₆ (12)	JW	13.2
	BK	13.9
H ₂ O(14)	JW	12.8
	BK	13.5
NH ₃ (16)	JW	35.0
	BK	22.2
N ₂ (20)	JW	33.1
	BK	24.6
C ₂ H ₂ (24)	JW	127
	BK	78.4
C ₂ H ₄ (28)	JW	261
	BK	222
CO ₂ (30)	JW	399
	BK	287

TABLE IV. The time used for training C-LBCS models for the results in Table I. The unit of time is second.